

Gasoline Vehicle Particle Size Distributions: Comparison of Steady State, FTP, and US06 Measurements

M. MATTI MARICQ,*
DIANE H. PODSIADLIK, AND
RICHARD E. CHASE

Ford Motor Company, Research Laboratory, P.O. Box 2053,
MD 3083, Dearborn, Michigan 48121

Factors influencing the number and size of tailpipe particles from port injection, spark ignition vehicles are examined by comparing emissions recorded during steady-state operation and those obtained from FTP and US06 drive cycles. Size distributions are measured using the scanning mobility particle sizer (SMPS) and the electrical low-pressure impactor (ELPI). Steady-state particulate emissions are examined as a function of vehicle speed and air to fuel ratio. The emission rates increase moderately with increasing speed but climb steeply with decreasing A/F. This is consistent with the observations from transient drive cycle measurements where particulate emissions occur predominantly during periods of heavy acceleration. As expected from the more aggressive speed and acceleration of the US06 cycle, the per mile particulate emission rates are higher than for phases 2 and 3 of the FTP. For the eight vehicles tested, the US06 mass emissions range from 1.2 to 9.6 mg/mi. Use of a US06-compliant calibration leads to a factor of 2 reduction of particulate emissions, in both number and mass, over the drive cycle.

Introduction

Recent epidemiological studies have raised concerns over the potential health effects of airborne particulate matter (1–3). The mechanism by which particles can adversely affect health is not yet understood; nonetheless, these concerns helped prompt the new ambient particle standard recently adopted by the Environmental Protection Agency (EPA) (4). The legislation introduces a separate criterion for ambient concentrations of fine particles, those below 2.5 μm in diameter ($\text{PM}_{2.5}$), to augment the existing PM_{10} standard. One premise for the new standard is the desire to classify different forms of particulate matter. Distinguishing two size cuts achieves this to some degree, because the fine particle mode arises primarily from combustion-related processes and gas to particle conversion processes, whereas the coarse mode particles, which generally dominate PM_{10} , originate largely from mechanical processes, windblown dust, etc.

Ambient particulate matter arises from a complex mixture of sources, one of which is tailpipe emissions from gasoline vehicles. While the contribution varies with location and season and from day to day, it represents roughly 10% of the $\text{PM}_{2.5}$ particulate mass in the Los Angeles region (5). Recent in-use vehicle tests reveal that older technology and malfunctioning vehicles contribute more of this fraction of

particulate matter and that newer technology vehicles contribute less (6, 7). The conventional determination of tailpipe PM emissions is mass based. Over the past few years, studies have begun to address the questions of particle size and number, thus far primarily under steady-state operation (8–12). We have been extending this to the second by second examination of particle emissions over transient drive cycles. The results obtained for a series of 21 recent model gasoline vehicles over the FTP drive cycle have been reported in a previous paper (13). The particles fall predominantly into the 10–300 nm diameter range and, thus, belong to the $\text{PM}_{2.5}$ category. However, we found the particulate mass emission rates to be very low, typically in the range of 1–2 mg/mi over the three-phase FTP drive cycle.

It has been recognized that the FTP cycle does not represent all driving conditions. The EPA, as part of the National Low Emitting Vehicle (NLEV) Program, has recently introduced the supplemental FTP cycle (14). One portion of the SFTP, the US06 cycle, addresses the issue of aggressive, high-speed driving; the other (SC03) is directed at the effect of operating the air conditioner on vehicle emissions. The new standards are based on gaseous emissions, with CO and a non-methane hydrocarbon (NMHC) plus NO_x category representing the two regulated emissions. To achieve compliance, vehicles must meet composite (35%FTP + 37%SC03 + 28%US06) levels of 0.65 g/mi NMHC + NO_x and 3.4 g/mi CO as well as maintain less than 9.0 g/mi CO over the US06 portion of the test. The standards are slated to be phased in beginning with the 2001 model year.

Ford is committed to meeting or exceeding environmental regulations; therefore, it is of interest to characterize particulate emissions over the US06 cycle and to examine the effect of US06 compliance on PM emission levels. One can speculate a variety of reasons why gasoline vehicle tailpipe particulate levels might increase over this drive cycle. These include the observation that particle emission rates correlate with vehicle acceleration (13). Also, the necessity of protecting the catalyst under high engine loads may lead to higher particle emissions. To understand better the issue of tailpipe particulate matter, this paper presents particle size, number, and mass measurements from the US06 drive cycle at high-speed steady-state driving and as a function of air to fuel ratio (A/F).

Experimental Methods

The particulate emissions measurements were carried out using the chassis dynamometer facility at the Vehicle Emissions Research Laboratory (VERL) of Ford Motor Company. A detailed description of this facility and the experimental procedures is given in a previous paper (13). The vehicles are run on a 48-in. single-roll dynamometer. The vehicle exhaust flows through a 9.1 cm diameter, 5.8 m long, heated (113 °C), corrugated, stainless steel tube to a 30.4 cm diameter dilution tunnel where it is turbulently mixed with dilution air. The transit time from tailpipe to dilution tunnel varies from about 20 s when the vehicle is idling to <1 s during heavy acceleration. The dilution air is filtered, reducing the particle number concentrations to nearly 1/10 that of ambient, dehumidified, and heated to 38 °C. Its flow is controlled to maintain a constant total flow (exhaust + diluent) of 10 standard m^3/min (corrected to 20 °C and 101 kPa) through the dilution tunnel for the FTP tests and 20 standard m^3/min for the US06 tests. Because the total flow is maintained constant, the dilution ratio varies from about 120 during idle to ~4 during the heaviest accelerations. The

* Corresponding author telephone: (313)594-7527; fax: (313)594-2923; e-mail: mmarricq@ford.com.

residence time of a particle in the tunnel is approximately 3 s at the 10 standard m³/min flow rate.

As a cautionary note, suspicious particulate emissions were sometimes observed in the course of the present study; for example, a manyfold rise in the tunnel background particle number that occurs after some US06 tests or order of magnitude higher particle emissions at a steady-state 40 mph cruise that follows, as compared to one that precedes, a test at 70 mph. Further investigation, discussed in detail in a separate publication (15), traces these "artifactual" emissions to the thermal desorption and/or pyrolysis of hydrocarbons (i) deposited on the wall of the transfer hose connecting the vehicle tailpipe to the dilution tunnel or (ii) from silicone rubber couplers used to connect the transfer hose to the tailpipe (not used in the present study). Both can cause apparent particle number emissions that are orders of magnitude higher than the actual gasoline vehicle tailpipe emissions. In the present experiments, the steady-state measurements illustrated below in Figure 3 are corroborated by particle size distributions measured directly from the tailpipe using an ejector pump diluter (Dekati Ltd., Tampere, Finland). In our US06 cycle measurements, the artifact effects were nonexistent or minor, possibly due to our use of separate transfer hoses and dilution tunnels for gasoline versus diesel fueled vehicles, but this may not be the case in all test facilities.

Particles for filter collection are sampled isokinetically, at 0.66 L/s, more than 10 tunnel diameters downstream from the mixing region. No means are used to limit the particles to PM₁₀, although this might be desirable when testing vehicles from which a few larger debris particles, for example, flaking from an old exhaust system, might skew the filter PM mass measurements. The particles are collected on 2-μm Teflo filters (Gelman Sciences, Ann Arbor, MI) for the US06 cycle and for each phase of the FTP drive cycle. For the US06 cycle, the mass is collected for each test. For the FTP, because of the low particulate levels, the emissions from four separate day's tests are integrated onto each filter in order to improve accuracy. After being allowed to equilibrate for a minimum of 2 h, the filters are weighed using a Cahn C-33 microbalance. The particulate mass, typically 5–500 μg, is corrected for background particulate matter (<1 μg) remaining in the filtered dilution air. The errors in the reported mass emission rates are approximately 0.1 mg/mi.

Number-based particle size distributions are determined using the scanning mobility particle sizer (SMPS) (TSI Inc., St. Paul, MN) and the electrical low-pressure impactor (ELPI) (Dekati Ltd., Tampere, Finland). The former instrument separates particles by size based on their electrical mobility. The latter charges the particles in a corona discharge and then records the electrical currents as the charged particles are separated according to aerodynamic size on various stages of a cascade impactor. For steady-state vehicle operation, the size distributions are recorded in the conventional manner. A scan time of 2 min was used for the SMPS in order to minimize distortion of the distributions. To record size distributions during the transient FTP and US06 drive cycles, the ELPI range was set to 400 pA to obtain the fastest time response (~1 s).

The minimum scan time of 30 s for the SMPS is too long to permit directly recording transient particle size distributions. Instead, these are constructed from particle number versus time traces taken at fixed particle size from a series of vehicle drive cycles. The number of particles transmitted through the electrostatic classifier of the SMPS, $C(t, D_p)$, is recorded at 2-s intervals using the 3010 condensation nuclei counter (with a time response of about 2 s). These counts per second are converted to a differential tailpipe emission

rate via

$$\frac{dN(t)}{d \log(D_p)} = \frac{C(t, D_p) T(D_p) q_T}{q_a f(+1) \epsilon_i \epsilon_c} e^{\alpha C} \quad (1)$$

Here $N(t)$ denotes the particles per second exiting the tailpipe, $T(D_p)$ is the transmission function of the classifier (approximated as a triangle, $2/\Delta(\log D_p)$), q_T is the tunnel flow, q_a is the aerosol sample flow, $f(+1)$ is the size-dependent fraction of particles with a single positive charge, and ϵ_i and ϵ_c are respectively the efficiencies of the condensation nuclei counter and the impactor at the entrance of the classifier. The factor $e^{\alpha C}$ represents a coincidence correction for high particle count rates ($\alpha = 4 \times 10^{-7}$ s).

Our previous study (13) showed very good reproducibility of particle emissions over a series of FTP cycles. It is not quite as good for the more demanding US06 cycle, presumably because of the increased difficulty in precisely following the more aggressive speed trace and the nonlinear dependence of particle emission rates on changes in vehicle speed and engine load. If necessary, the ELPI data can be used to ascertain the reproducibility of the individual US06 tests, and the SMPS particle number versus time traces can be corrected.

Either EPA certification fuel or California Phase II reformulated fuel was used in this study. For the FTP tests, each vehicle was prepared by being run through the drive cycle and then soaked overnight. Particulate emissions data were collected on the subsequent 4 days, with the vehicle run through one FTP cycle per day, due to the necessity of a cold start. Between tests, the filters in their holders were kept in sealed plastic bags. US06 tests were performed in groups of 3–5 per day, with the first test used to warm the vehicle. Steady-state tests were conducted after the vehicle was run through at least phase 1 of the FTP cycle to bring it to operating temperature. Neither the US06 nor steady-state tests were interspersed with a series of FTP tests.

Results

The vehicles used in the present study are described in Table 1. All are recent model, port injection, gasoline-fueled vehicles except for the European diesel, which is used for the purpose of comparison. The gasoline-fueled vehicles are all equipped with a three-way catalyst, except for vehicle T4, which is used to examine the effect of A/F on particle emissions. Most of the vehicles are low mileage (<10 K); one has an odometer reading of >100 K miles. Table 2 gives the gas-phase emissions for the test vehicles over the US06 and FTP drive cycles; here the FTP numbers represent the conventional weighted three-phase average. The gaseous emissions indicate the operating condition of the test vehicles and help put the particulate emissions in perspective.

US06 Particulate Emissions. Figure 1 compares number-weighted size distributions of particles recorded over the US06 cycle from a variety of the test vehicles to those measured during phases 1 and 3 of the FTP (note that some of the data are scaled for clarity). For three of the example vehicles, particle emissions during the US06 lie intermediate between those of phases 1 and 3 of the FTP. For the fourth example, the US06 particle numbers are about 3 times higher than those for phase 1. Phases 1 and 3 of the FTP both follow the same speed trace; they differ in that phase 1 requires a cold start, whereas phase 3 occurs after a 10-min hot soak. The correlation between particle emissions and vehicle acceleration, which has been observed both in our previous work (13) and here, suggests that the US06 particle emissions are higher than those of phase 3 because of the more aggressive accelerations and higher speeds demanded by

TABLE 1. Description of Vehicles and Tests

vehicle ^a	year	cyl	test fuel	odometer miles	transmission	test type
T1	1997	6	EPA certified	35 500	automatic	FTP, US06
T2	1997	6	CA ph 2 refrm ^b	4 200	automatic	FTP, US06
T3a	1996	6	CA ph 2 refrm	5 450	automatic	FTP, US06
T3b	1996	6	CA ph 2 refrm	2 900	automatic	FTP, US06
C1	1997	6	CA ph 2 refrm	3 500	automatic	FTP, US06
C2	1996	4	CA ph 2 refrm	5 660	automatic	FTP, US06
C3	1996	8	CA ph 2 refrm	<6 000	automatic	FTP, US06, ss
C4	1998	8	CA ph 2 refrm	104 000	automatic	FTP, US06
T4	1995	6	EPA certified	2 600	automatic	steady state
C5	1997	4	CA ph 2 refrm	5 350	automatic	steady state
EC	1997	4	Euro ref	2 000	automatic	steady state
diesel	1995	4	Euro, 0.034 wt % sulfur	12 200	5 spd manual	steady state

^a T, light-duty truck; C, passenger car; EC, European car. ^b California Phase 2 reformulated.

TABLE 2. Average Regulated Gaseous Emissions

vehicle	test	THC (g/mi)	CO (g/mi)	NO _x (g/mi)	CO ₂ (g/mi)
T1	FTP	0.081	1.35	0.049	451.2
T1	US06	0.031	14.3	0.101	419.8
T2	FTP	0.091	0.90	0.094	421.7
T2	US06	0.057	5.49	0.200	485.8
T3a	FTP	0.092	1.06	0.077	506.8
T3b	FTP	0.151	1.12	0.165	542.9
T3b	US06	0.107	5.05	1.132	638.1
C1	FTP	0.183	0.96	0.045	457.1
C1	US06	0.113	10.3	0.061	459.1
C2	FTP	0.073	1.08	0.080	314.0
C2	US06	0.183	35.7	0.078	360.9
C3	FTP	0.085	0.91	0.060	464.6
C4	FTP	0.180	1.37	0.198	457.0
C4	US06	0.055	3.42	0.471	471.4
diesel	FTP	na ^a	0.49	0.741	306.4

^a na, not available.

the US06 cycle. Likely, they are smaller than for phase 1 of the FTP cycle because of the cold start used for phase 1.

The particle emissions can be characterized according to number, geometric mean size, and standard deviation of size by fitting the distributions to a log-normal form:

$$f(\ln(D_p)) = \frac{N}{\sigma 2^{1/2} \pi^{1/2}} \exp[-(\ln(D_p) - \ln(\mu))^2 / (2\sigma^2)] \quad (2)$$

This description is often a good approximation to the experimentally measured size distribution. Here, it effectively allows us to interpolate between the coarse grid of particle sizes necessary for recording transient particle emissions using the SMPS. μ is the geometric mean diameter, σ is the standard deviation, and N is the number of particles emitted from the tailpipe during the specified test. By weighting the distribution according to particle volume and density and integrating over diameter, the mass of particles emitted is found to be

$$M_T = \frac{N \rho \pi}{6} \mu^3 \exp(9\sigma^2/2) \quad (3)$$

with ρ representing the particle density. Although it varies with particle size (1θ), the density is assumed to equal 1 g/cm³ for the purpose of making a rough comparison to the tailpipe PM collected on filters. For the vehicles in this study, the parameters characterizing the particle distributions and the masses deduced from these distributions are collected in Table 3 along with the mass emission rates measured by filter collection.

As evident from Figure 1 and Table 3, the particles emitted during the FTP predominantly fall into the 10–300 nm

diameter range, with a number-weighted geometric mean of about 60 nm. Depending on one's definition of ultrafine particles, a significant fraction of the particles fall into this category. Assuming ultrafine particles to be those falling below a certain cutoff diameter, e.g., 50 nm, their number can be estimated from the size distributions in Figure 1; thus, roughly 40% of the FTP particle emissions fall below 50 nm. For mass-weighted distributions, the mean shifts to about 200 nm because of the D_p^3 dependence of particle mass.

The mean sizes of particles from phase 1 are about 10 nm larger than for phase 3 (see also ref 13); however, the particle numbers during phase 1 are higher by a factor of 5–100. The filter-based mass emissions exhibit the same trend, although the phase 1 to phase 3 particle mass ratios are not as large as those for particle number. Within the 50–100% error bars incurred in converting particle size data to mass emission rates, the calculated masses are in good agreement with those based on gravimetric measurements. This agreement is taken as evidence that the masses collected on the filters originate from the combustion-related fine and ultrafine particles and are not due to other fine or coarse mode debris exiting the tailpipe.

The situation is somewhat different for the US06 cycle. The number-weighted mean particle diameter falls to below 40 nm for five of the test vehicles (see Figure 1 and Table 3); for two vehicles, it remains in the 50–70 nm range. Consequently, the fraction of ultrafine (<50 nm) particles increases to roughly 60%. The US06 mass emission rates per mile, as determined by filter collection, increase by a factor of 6–30 over the emissions from phase 3 of the FTP (see Table 3); however, this is largely because the FTP phase 3 emissions are nearly negligible. The increase with respect to total particle number is larger, varying from a factor of 12 to 180. One reason for the larger ratio is that, unlike the mass emission rates, the total numbers of emitted particles reported in Table 3 are not normalized by the distance of the drive cycle (8.0 mi for the US06 versus 3.6 mi for phase 3 of the FTP). Another reason for the larger US06 to FTP particle number ratio is the decrease of particle size for the US06 versus FTP cycle.

In contrast to the FTP results, Table 3 shows that the US06 mass emissions calculated from the particle size distributions for some vehicles are vastly smaller than the filter-based mass measurements. Notable examples are vehicles T3a, T3b, and C1. The reasons for the discrepancies are unclear. Our assumption that the particle density is 1 g/cm³ could be partly responsible; however, this would require that the density be different for the FTP and US06 PM emissions since acceptable agreement between calculated and filter-based PM mass is found for the FTP tests. For each of vehicles T3a and T3b, one of the repeat US06 gravimetric PM determinations measured over 4 times the

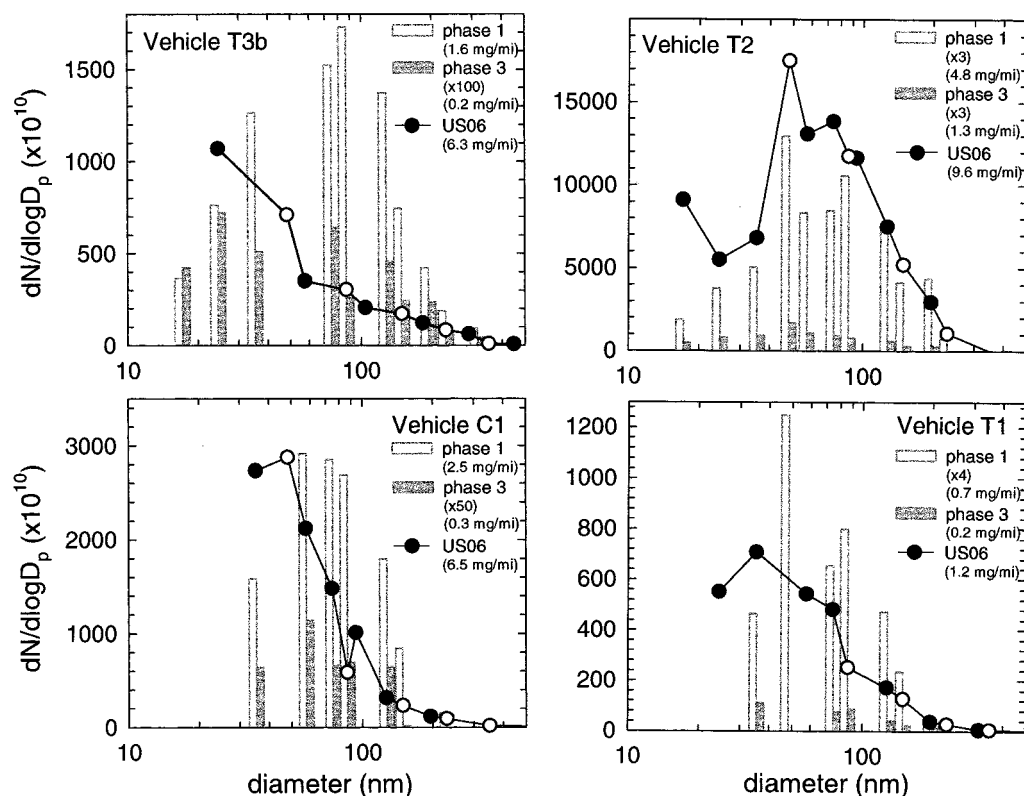


FIGURE 1. Comparison of particle size distributions integrated over the US06 drive cycle to those integrated over phases 1 and 3 of the FTP. The US06 data are shown via the symbols and connecting lines, with filled symbols denoting SMPS data and open symbols representing ELPI data. The mass emission rates that are provided are the filter-based values from Table 3.

average mass, possibly biasing the mass emission rate. This could happen if “large”, micrometer-sized, particles are sporadically shaken loose from the exhaust system or transfer line, which would be missed by the particle number measurements. However, this cannot be the entire reason, since even when omitting the outliers the filter masses remain considerably higher than the masses calculated from the size distributions. Another possibility is that gaseous hydrocarbons are adsorbed by the filter medium; however, the hydrocarbon emissions for the vehicles in question are not particularly higher than those of the other test vehicles (Table 2) nor higher than for the FTP cycle, for which good agreement was generally obtained between gravimetric and particle number-derived mass emission rates.

Transient particle size distributions from the US06 and phase 3 of the FTP drive cycles are compared in Figure 2 (top graphs). The contrast between the two drive cycles appears stark because the phase 3 FTP particle emissions for the test vehicle (C1) remain near the tunnel background level. The phase 3 emission of 1.2×10^{11} particles reported in Table 3 for vehicle C1 is only 2.4 times higher than the 5×10^{10} particles that would be measured upon introducing a quantity of ambient air equal to the exhaust volume into the dilution tunnel. For both drive cycles, particle emissions are correlated with vehicle acceleration. Aside from the emission events at $t = 0$ s and $t = 180$ s during the FTP test, other, weaker emissions can be observed for the three accelerations over the 300–500 s range upon expanding the vertical scale. The fact that particle emissions are more apparent during the US06 cycle, with more aggressive accelerations, suggests that changes in fuel injection, vaporization, A/F ratio, and mixing during these transient events are responsible for the higher particle numbers.

As discussed previously (13), the rate of particles exiting the tailpipe during acceleration increases for two reasons: first, simply because the exhaust flow increases and, second,

because the efficiency of particle formation increases due to in cylinder changes in particle formation and oxidation processes that occur during acceleration. The lower traces in Figure 2 of air to fuel ratio support the second idea, namely, that the particle concentration in the exhaust increases. During phase 3 of the FTP, the A/F remains near stoichiometry, and very low particle emissions are observed. The same is true for carbon monoxide. For the US06, the particle emissions as well as CO emissions correlate with rich excursions of the A/F. Thus, the increased particulate matter levels during heavy accelerations are due not only to an increase in exhaust flow, but changes in the combustion process are also responsible. For other test vehicles, the correlation between particle emissions and A/F is not as clear as in Figure 2, which suggests that rich excursions are not the sole mechanism for increases in exhaust particle concentrations.

Steady-State Measurements. The correlations observed between particle emission rates, vehicle acceleration, and carbon monoxide emissions suggest that vehicle speed, load, and A/F are important quantities relevant to the particle formation and oxidation processes. To explore this further, a separate series of experiments was carried out in which some of the test vehicles were run under various conditions of constant speed and horsepower. Figure 3 compares the particle emissions from three gasoline vehicles and one light-duty diesel-powered automobile as a function of speed (note that the vertical scales are not all identical). Each vehicle was run using its normal dynamometer coefficients; thus, the test is equivalent to a constant speed cruise on a flat roadway with no wind. As the speed increases, so does the load on the engine due to the higher air resistance that must be overcome.

The three gasoline vehicles in Figure 3 exhibit qualitatively similar trends in particle emissions as a function of speed. Up to about 40 mph, exhaust particles at a steady cruise are virtually nonexistent; there are on the order of 10^8 particles/s

TABLE 3. Particulate Matter Emissions

vehicle	phase ^a	$N (\times 10^{12})$ (no./test)	mean diam. ^b (nm)	σ^c	M_f (mg/mi)	filter ^d (mg/mi)
T1	1	23 ± 7	66 ± 8	0.6 ± 0.1	4 ± 3	0.7
	2	0.6 ± 0.2	61 ± 11	0.7 ± 0.2	0.1 ± 0.1	0.1
	3	0.9 ± 0.2	45 ± 9	0.7 ± 0.2	0.1 ± 0.1	0.2
	US06	5.2 ± 0.6	38 ± 6	0.7 ± 0.1	0.2 ± 0.1	1.2
T2	1	24 ± 4	71 ± 9	0.7 ± 0.1	10 ± 9	4.8
	2	0.5 ± 0.2	45 ± 17	0.9 ± 0.4	0.3 ± 0.5	0.4
	3	3.1 ± 0.3	47 ± 5	0.8 ± 0.1	0.8 ± 0.5	1.3
	US06	135 ± 17	53 ± 5	0.6 ± 0.1	8 ± 4	9.6
T3a	1	2.7 ± 0.7	49 ± 8	0.6 ± 0.2	0.3 ± 0.4	0.9
	2	0.2 ± 0.2	61 ± 32	0.7 ± 0.7	0.04 ± 0.15	0.1
	3	0.4 ± 0.1	84 ± 15	0.4 ± 0.3	0.06 ± 0.04	0.3
	US06	4 ± 3	25 ± 20	0.9 ± 0.4	0.2 ± 0.6	6.0 ^f
T3b	1	14 ± 2	63 ± 6	0.7 ± 0.1	5 ± 3	1.6
	2	0.07 ± 0.03	51 ± 20	0.9 ± 0.4	0.2 ± 0.5	0.1
	3	0.07 ± 0.02	37 ± 15	1.0 ± 0.4	0.1 ± 0.1	0.2
	US06	3.6 ^e	<30		0.4 ^e	6.3 ^f
C1	1	18 ± 2	67 ± 4	0.6 ± 0.1	2 ± 1	2.5
	2	0.12 ± 0.06	80 ± 13	0.5 ± 0.2	<0.1	0.1
	3	0.12 ± 0.06	57 ± 18	0.6 ± 0.3	<0.1	0.3
	US06	16 ± 3	40 ± 5	0.5 ± 0.1	0.3 ± 0.2	6.5
C2	1	4.1 ± 1.0	66 ± 10	0.6 ± 0.2	0.4 ± 0.4	0.4
	2	0.3 ^e			0.08 ^e	0.1
	3	0.7 ^e			0.34 ^e	0.3
	US06	1.6 ^e	<35		0.4 ^e	1.4
C3	1	2.6 ± 0.3	64 ± 5	0.5 ± 0.1	0.3 ± 0.1	0.9
	2	0.07 ± 0.02	60 ± 8	0.7 ± 0.1	0.02 ± 0.01	0.7
	3	3.1 ± 0.4	107 ± 10	0.3 ± 0.2	0.7 ± 0.3	0.5
	US06	10 ± 2	70 ± 8	0.3 ± 0.1	0.3 ± 0.1	
C4	1	6.6 ± 1.0	50 ± 10	0.8 ± 0.2	0.8 ± 0.9	1.1
	2	0.02 ^e			<0.1 ^e	0.1
	3	0.05 ± 0.02	50 ± 10	1.1 ± 0.6	<0.1 ^e	0.3
	US06					5.0 ^f

^a FTP data from ref 13. ^b Mean of log-normal particle size distribution (eq 1), equivalently geometric mean size, with 95% confidence limits.

^c Standard deviation (width) of log-normal size distribution with 95% confidence limits. ^d The estimated measurement uncertainty is ±0.1 mg/mi.

^e Mass obtained by numerical integration of measured size distribution—not by fitting to a log-normal distribution. ^f Includes an outlier of more than 4 times the average mass.

emitted, implying an exhaust concentration of $\sim 7 \times 10^3$ particles/cm³. This is consistent with the observed lack of particle emissions between accelerations during constant speed portions of the transient drive cycles (Figure 2). Beginning around 50 mph, particle emissions are observed in the 20–30 nm region. Since the exhaust flow at 70 mph is barely twice the flow at 50 mph, there is an increase in exhaust particulate matter concentration that must arise from the combustion process. Despite the increase in particle number, the mass emissions remain very low, well less than 0.1 mg/mi even at 70 mph. To put this in perspective, the PM emissions from a diesel vehicle are roughly 3 orders of magnitude higher, both in particle number and in mass.

One implication of the steady-state measurements is that the increase in average vehicle speed between the FTP and US06 cycles is unlikely to explain the difference in particle emission rates noted in Figure 1. The engine load required to overcome vehicle inertia during acceleration is generally higher than the load needed to overcome air resistance even at 70 mph; thus, this could contribute to the larger US06 particle emissions. Alternatively, transient changes in engine operating conditions, such as in the air to fuel ratio, are responsible for the larger PM emissions.

It is pertinent to note here that steady-state measurements performed with a vehicle on a chassis roll, as opposed to those utilizing an engine dynamometer, are not always steady. As the vehicle speed is increased toward 70 mph, substantial fluctuations can be observed both in the amplitude and shape of the particle size distributions. Some of these may originate from the fact that, even at a steady speed, the engine control electronics can momentarily alter the engine operating parameters. Another cause of inconsistent steady-state PM

emissions is the existence of particle emissions artifacts that arise from transporting the hot vehicle exhaust from tailpipe to dilution tunnel, as discussed in the Experimental Methods section above and detailed in ref 15.

One operating condition that has a large impact on particle formation is the A/F ratio. Figure 4 illustrates the changes in particle size distributions as the ratio is varied from stoichiometry; $\lambda = 1$ toward rich mixtures, $\lambda < 1$. The corresponding gaseous emissions and calculated particulate mass emissions are also provided in the figure. The repeat traces within each panel indicate the test – test variability. The size distributions are all plotted on a 0–20 vertical scale, but there is an exponent associated with each panel. Decreasing λ from stoichiometric to 0.9 produces a 2–3-fold increase in particles. The size distribution narrows somewhat but remains centered at 50–60 nm diameter. Reducing λ to 0.85 leads to a nearly 10-fold increase in particle number and a slight additional narrowing of the distribution. A further reduction of λ to 0.8 causes another 10-fold increase in particle emissions, but there is an accompanying increase in the breadth of the distribution.

If the size distributions are integrated over particle diameter, then the total particle number emission rate versus air to fuel ratio varies approximately as $N = 8.1 \times 10^8 \exp[160(1 - \lambda)^2]$, as depicted in Figure 5. It is worth noting that during the peaks in particle emission that occur in the US06 cycle (see Figure 2) the rich excursions of A/F approach a value of $\lambda = 0.8$. At this air to fuel ratio, Figure 5 indicates a ~ 300 -fold increase in particles relative to stoichiometric operation, which is consistent with the peaks in the transient particle emissions.

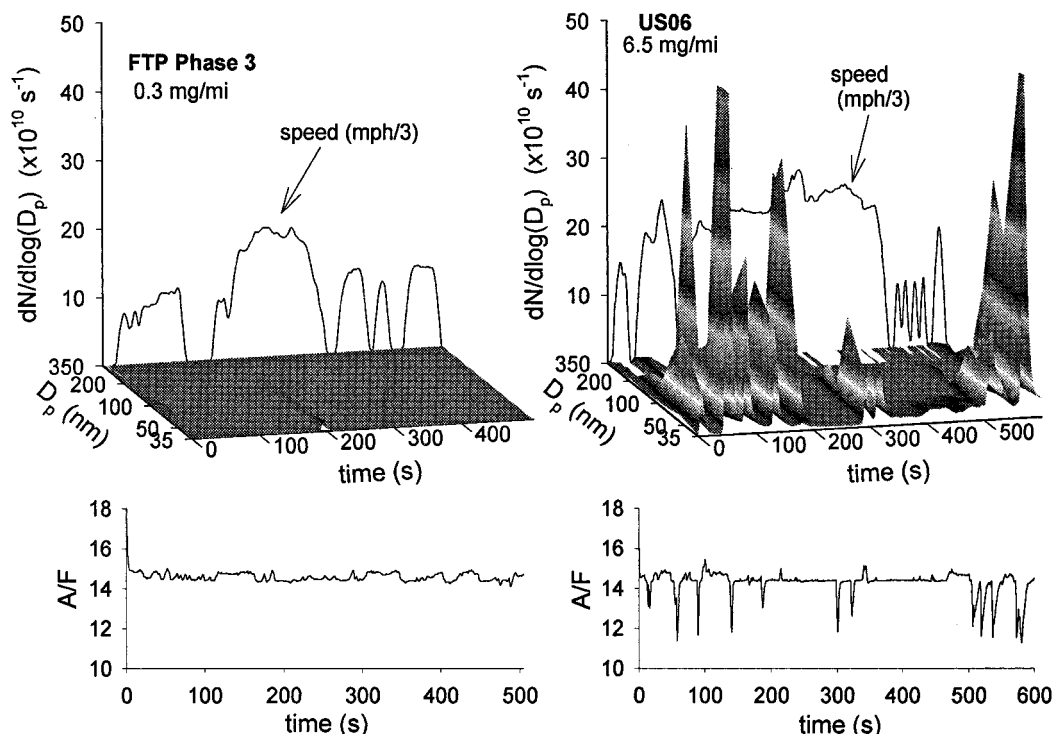


FIGURE 2. Comparison of transient particle size distributions from phase 3 of the FTP and the US06 drive cycles for vehicle C1. The respective speed traces are shown along the rear of the upper graphs. The lower plots show the variation in the air to fuel ratio during the drive cycles.

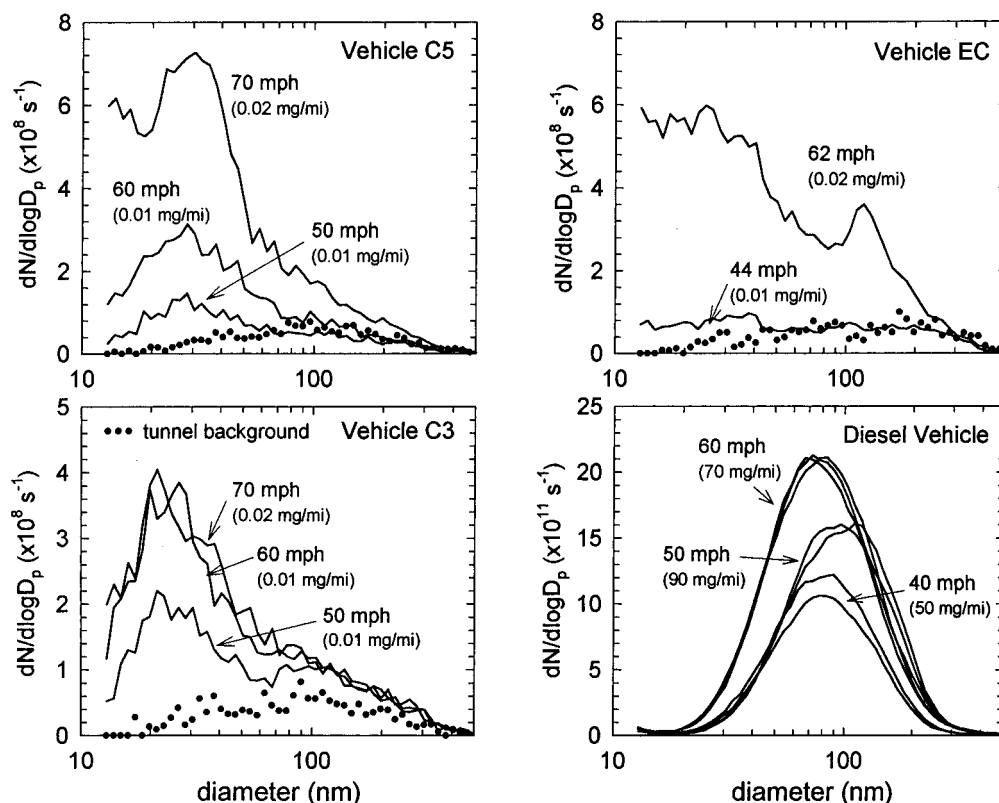


FIGURE 3. Dependence of particle emissions on vehicle speed for vehicles C5, EC, and C3 and the diesel vehicle (note that the vertical scale for the diesel vehicle is 1000 times larger than for the gasoline vehicles). Multiple lines within a group show variations over repeated tests under the same conditions. Symbols denote the size distribution of particles in the dilution air. These background particles have not been subtracted from the vehicle data. Exhaust flows for vehicle C5 are 0.010, 0.014, and 0.020 m³/s at 50, 60, and 70 mph. For vehicle C3, they are 0.014, 0.019, and 0.026 m³/s. Mass emission rates are estimated from the size distributions.

It is interesting to compare the trends in particulate versus engine-out gaseous emissions (listed in Figure 4). The falling NO_x levels are consistent with a decrease in combustion

temperature with lower λ . The hydrocarbon emissions show relatively modest increases as the air to fuel ratio becomes richer. The particulate levels more closely follow the trends

Particle emission vs A/F

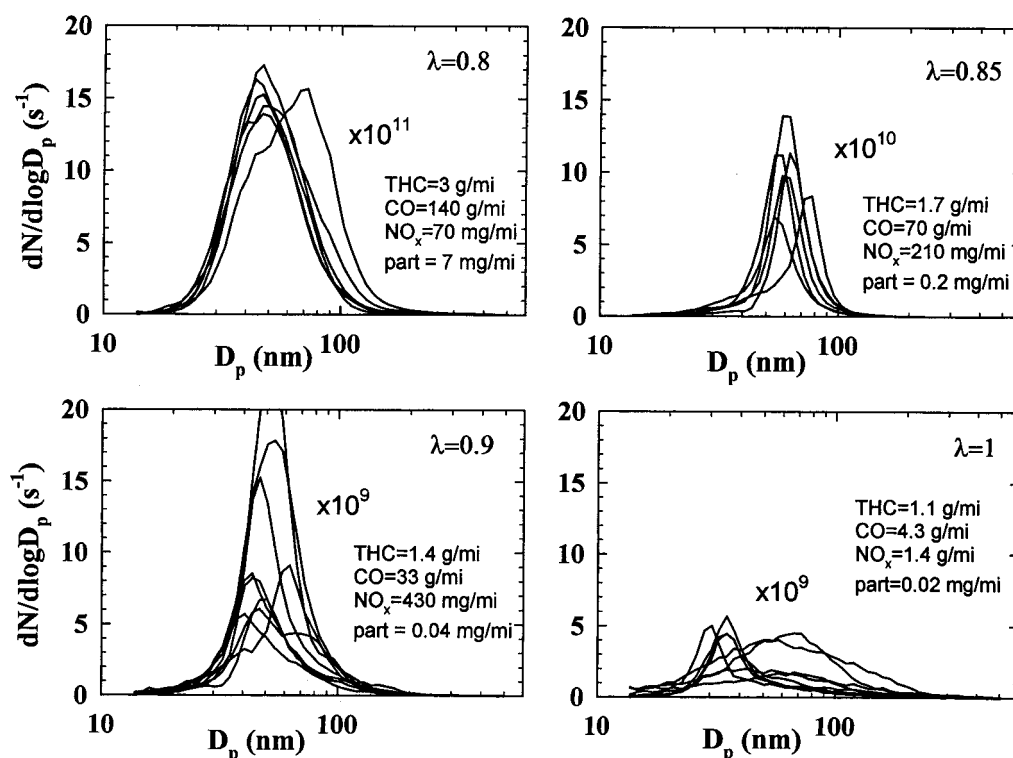


FIGURE 4. Particle size distributions as a function of λ (the ratio of A/F to its stoichiometric value) for vehicle T4. The vehicle speed is 50 mph. To convert from tailpipe particles/s to exhaust particle number concentration, divide by the exhaust flow of 1.4×10^4 cm³/s. Mass emission rates are estimated from the size distributions.

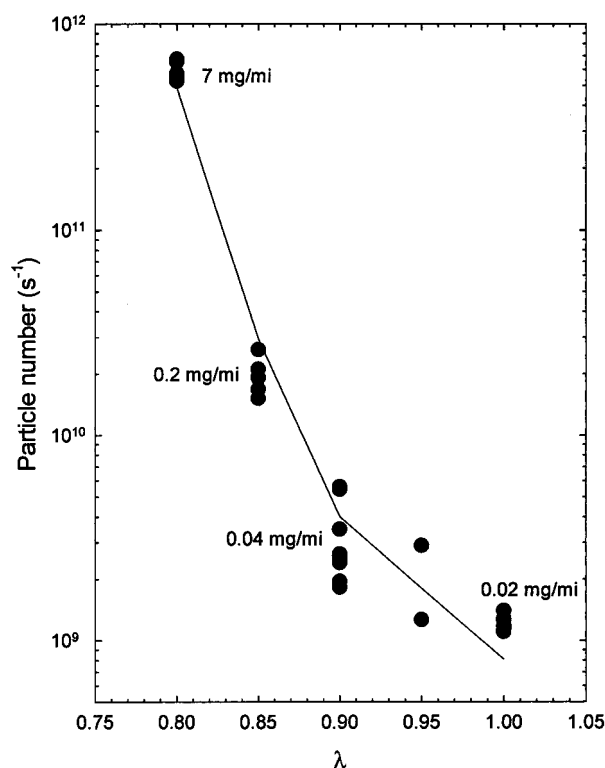


FIGURE 5. Particle number (and estimated mass) emission rates as a function of λ (the ratio of A/F to its stoichiometric value) for vehicle T4. The solid line shows the fit by $N = 8.1 \times 10^8 \exp[160(1 - \lambda)^2]$ particles/s.

in λ exhibited by CO emissions. A plausible reason for this is that engine-out hydrocarbon emissions contain both

incomplete combustion products as well as unburned fuel. In contrast, both CO and particles arise only from combustion.

Particle Emissions and US06 Compliance. One vehicle, T1, was tested both with the production engine calibration and using a US06-compliant calibration. The transient size distributions and accompanying mass emission rates are compared in Figure 6. It is apparent that the US06-compliant calibration reduces particulate emissions. Particle number emissions are approximately halved. The mean particle size and the width of distribution remain roughly the same. This is consistent with filter-based PM mass measurements, which also decrease by about a factor of 2 for the US06 calibration.

Discussion and Conclusion

As the results in the present paper illustrate, particle formation by spark ignition engines is a sensitive and nonlinear function of a number of operating parameters. The current work examines how the number and size of the emitted particles vary with drive cycle, vehicle speed, and air to fuel ratio. There are certainly many more parameters that influence the level of particulate matter in the exhaust, such as spark timing, fuel injector design, burn rate, etc. However a complete study of how these affect particle formation is clearly beyond the scope of this paper.

For port injection gasoline vehicles that are run over a moderate drive cycle, such as the FTP 3 phase or ECE cycle, particles are generated during vehicle acceleration and during the cold start. After catalyst light-off, particle emissions diminish to near negligible levels at moderate cruise speeds and during deceleration. This is evident both from the transient tests shown in Figure 2 and from the steady-state measurements illustrated in Figure 3. It is consistent with the low values of both particle number and mass recorded during phases 2 and 3 of the FTP (Table 3). The number-

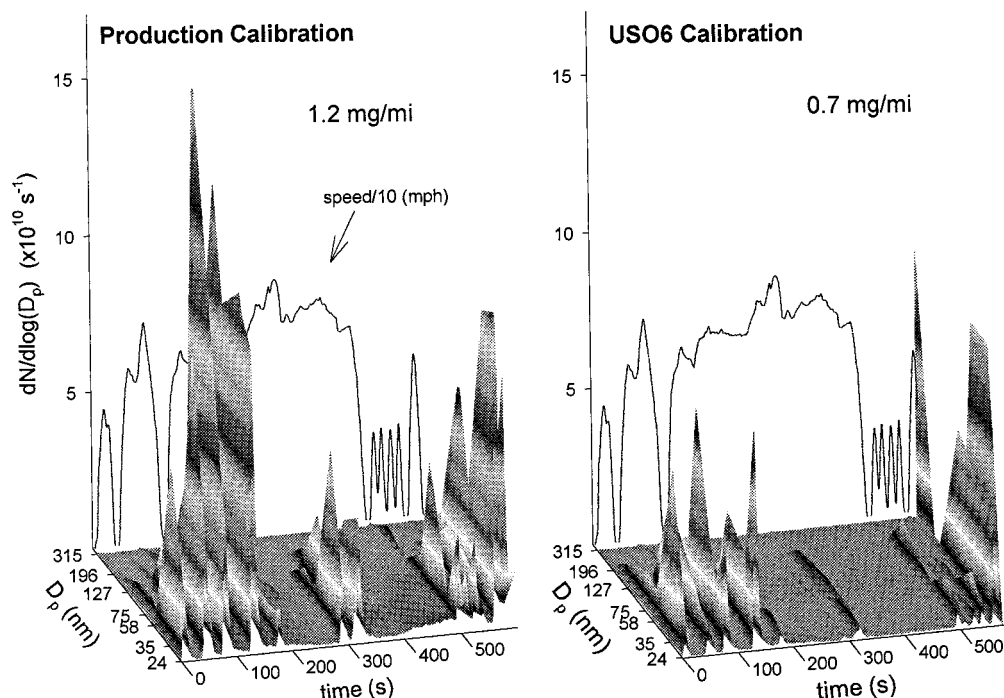


FIGURE 6. Comparison of US06 cycle particulate emissions using a production vs US06 compliant engine calibration.

weighted mean particle diameters fall into the 50–70 nm range and are relatively insensitive to the specific vehicle or phase of test. There is a reasonable consistency between the particulate masses deduced from the size distributions and those obtained from gravimetric measurements, which indicates that the mass collected by the filters actually derives from particles in the 10–300 nm range and not from a small number of much larger coarse mode particles.

Particle emissions from gasoline vehicles increase for the US06 portion of the supplemental FTP. The increase appears dramatic as compared to the very small FTP phase 3 emissions, but they remain below 10 mg/mi, and for a number of the test vehicles are comparable to FTP phase 1 emissions. They remain correlated with vehicle acceleration; thus, one cause of the increased emissions is the more aggressive nature of the drive trace. Changes in acceleration rates and vehicle speed, however, involve more than one engine parameter. During acceleration, both engine rpm and load change along with other quantities such as A/F and spark timing. The correlation in Figure 2 between A/F and particle emissions during the US06 indicates rich combustion to be one source of the particulate matter. This is verified by the steady-state measurements made under controlled variation of the A/F, which reveal a roughly $\exp[160(1 - \lambda)^2]$ phenomenological dependence of particle number emissions on λ .

Although no particle composition studies were carried out as part of the present study, some tentative conclusions can be drawn about the origin of the tailpipe particulate matter. Possible sources include soot from incomplete combustion of fuel and/or oil, ash from fuel and oil additives, and engine wear. The composition of the near background level particle emissions that occur between accelerations and at moderate steady cruise is unknown. However, the emissions that occur during acceleration, i.e., at the peaks along the drive cycle in Figure 2, most likely arise from incompletely burned fuel. While engine wear and the consumption of oil and the additives in fuel and oil are expected to increase during acceleration, it is unlikely that these increases would be sufficiently large to account for the increases in particles that occur under these driving conditions. Even at a nominally stoichiometric A/F, increases in soot formation could arise

from incomplete vaporization of the fuel droplets and/or incomplete mixing of the air–fuel mixture prior to ignition.

As stated in the Introduction, concern that the FTP driving cycle is not representative of current driving habits has led to the introduction of the SFTP cycle. For properly functioning current technology gasoline vehicles, particulate matter emissions remain low (<10 mg/mi) both at high speed and over the US06 drive cycle. It further appears that engine calibration changes made to achieve US06 compliance, which is based on the gaseous emissions, may further reduce this level by roughly a factor of 2.

The results presented here go beyond the traditional measurement of particle mass. The numbers, sizes, and transient responses of the exhaust particles can help point to engine design considerations that further reduce emissions. These issues need to be understood in order that future improvements in fuel efficiency or engine performance do not come at the expense of elevated particulate emissions. Ultimately, the important questions concern how the exhaust particles contribute to the overall atmospheric particulate load and how they impact the environment. A more thorough knowledge of the nature of motor vehicle particle emissions should help us address these questions.

Acknowledgments

We appreciate the excellent work of Mike Loos, Adolfo Mauti, and Jim Weir in setting up the dilution tunnel sampling systems and running the chassis dynamometer tests; of Dezi Lewis in determining the filter masses; and of Gary Dusz-kiewicz in calculating and compiling the mass emissions data. We thank Steve Japar and Ted Jensen for their help and support during this investigation.

Literature Cited

- (1) Dockery, D. W.; Pope, C. A. *Annu. Rev. Public Health* **1994**, *15*, 107–132.
- (2) Pope, C. A.; Bates, D. V.; Raison, M. E. *Environ. Health Perspect.* **1995**, *103*, 472–480.
- (3) Vedal, S. *J. Air Waste Manage. Assoc.* **1997**, *47*, 551.
- (4) National Ambient Air Quality Standard for Particulate Matter: Final Rule. *Fed. Regist.* **1997**, *62*, 38652.

- (5) Cass, G. R. Contribution of vehicle emissions to ambient carbonaceous particulate matter—review and synthesis of the available data in the south coast air basin. Report to the Coordinating Research Council, February 1997.
- (6) Cadle, S. H.; Mulawa, P.; Hunsanger, E. C.; Nelson, K.; Ragazzi, R. A.; Barrett, R.; Gallagher, G. L.; Lawson, D. R.; Knapp, K. T.; Snow, R. Light-Duty Motor Vehicle Exhaust Particulate Matter Measurements in the Denver, Colorado Area. In *PM_{2.5}: A Fine Particle Standard*; Chow, J., Koutrakis, P., Eds.; Air & Waste Management Assoc.: Pittsburgh, 1998; p 539.
- (7) Truex, T. J.; Durbin, T. D.; Smith, M. R.; Norbeck, J. M. Exhaust Particulate Emission Rates from In-Use Light-Duty Vehicles in the South Coast Air Quality Management District. In *PM_{2.5}: A Fine Particle Standard*; Chow, J., Koutrakis, P., Air & Waste Management Assoc.: Pittsburgh, 1998; p 559.
- (8) Greenwood, S. J.; Coxon, J. E.; Biddulph, T.; Bennett, J. *SAE Pap.* **1996**, No. 961085.
- (9) Rickeard, D. J.; Bateman, J. R.; Kwon, Y. K.; McAughey, J. J.; Dickens, C. J. *SAE Pap.* **1996**, No. 961980.
- (10) Maricq, M. *HEI Workshop on the Formation and Characterization of Particles*; HEI Communication No. 5; 1997.
- (11) Graskow, B. R.; Kittelson, D. B.; Abdul-Khalek, I. S.; Ahmadi, M. R.; Morris, J. E. *SAE Pap.* **1998**, No. 980528.
- (12) Morawska, L.; Bofinger, N. D.; Kocis, L.; Nwankwoala, A. *Environ. Sci. Technol.* **1998**, 32, 2033.
- (13) Maricq, M. M.; Podsiadlik, D. H.; Chase, R. E. *Environ. Sci. Technol.* **1999**, 33, 1618–1626.
- (14) Environmental Protection Agency. Proposed Rules, 40 CFR Part 86. *Fed. Regist.* **1997**, 62, 44753.
- (15) Maricq, M. M.; Chase, R. E.; Podsiadlik, D. H.; Vogt, R. *SAE Pap.* **1999**, No. 1999-01-1461.
- (16) Ahlvik, P.; Ntziachristos, L.; Keskinen, J.; Virtanen, A. *SAE Pap.* **1998**, No. 980410.

Received for review September 29, 1998. Revised manuscript received March 24, 1999. Accepted March 29, 1999.

ES981005N